Accurate and efficient boundary integral computations for interfacial flow with surfactant

Michael Siegel, NJIT

Collaborators:
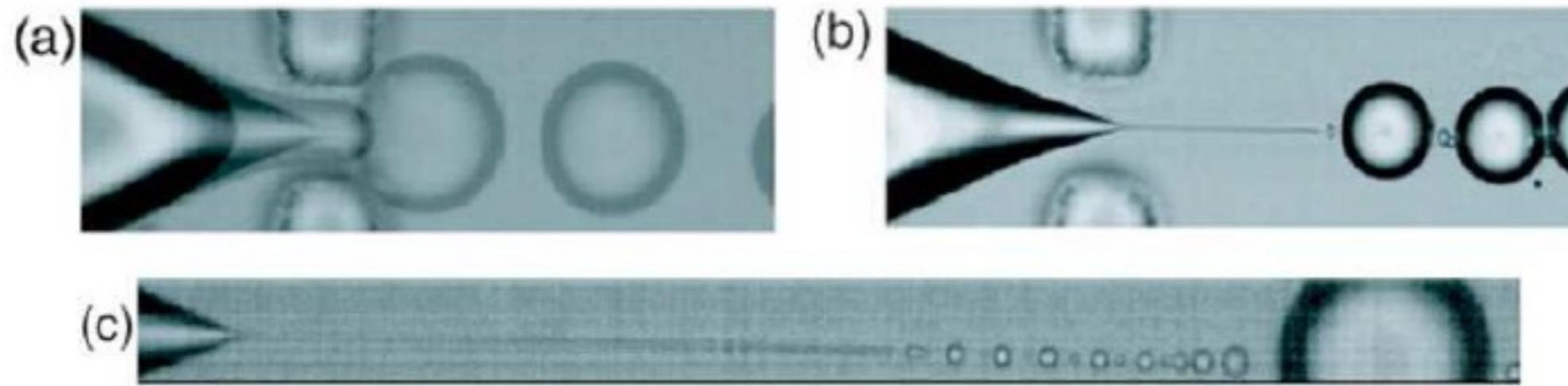
Project 1. Michael Booty (NJIT), Jacek Wrobel (Tulane), Qiming Wang (NJIT)

Project 2. Sara Palsson and Anna-Karin Tornberg (KTH, Stockholm)
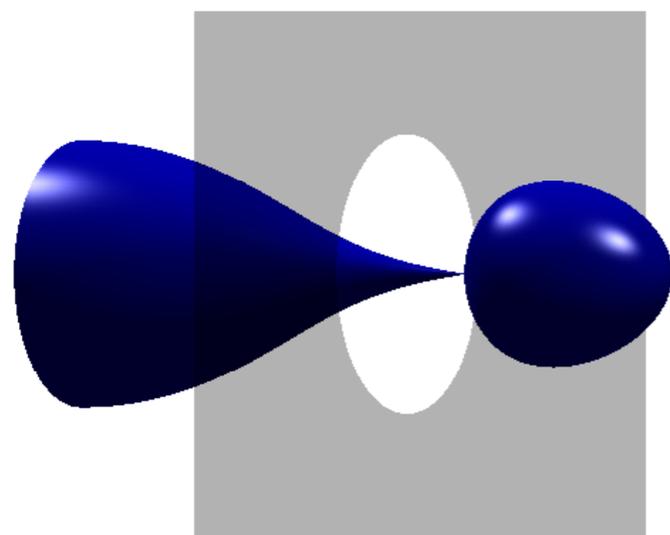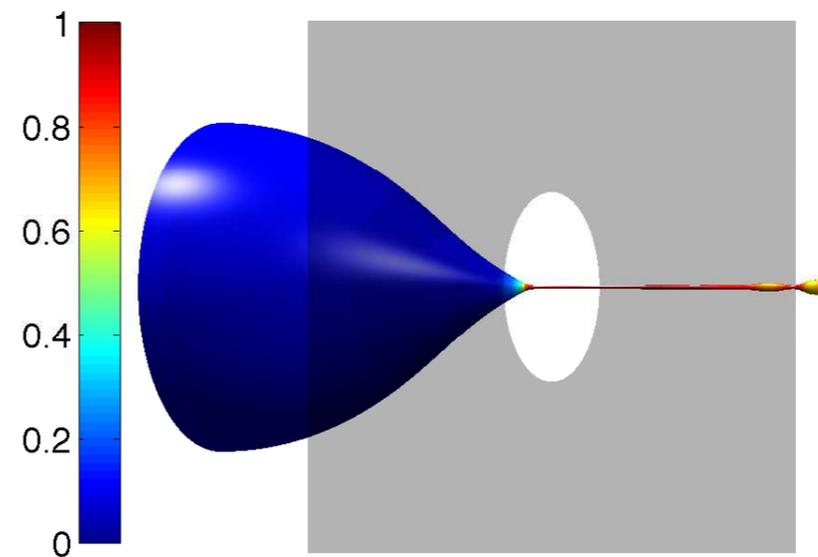
Tipstreaming in a microfluidic flow focussing device

Anna and Meyer 2006: Tipstreaming in a flow focusing device.
The orifice is 34 micrometers. (Related work by H. Stone, T. Ward, Moyle et al.)

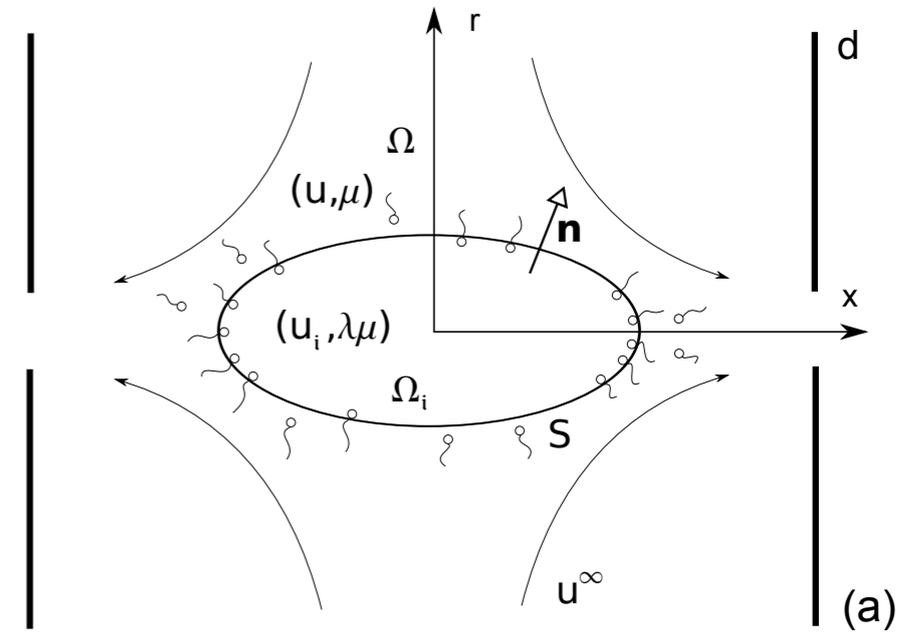

No surfactant

Insoluble surfactant

Numerical challenges

- Small diffusion: there is a narrow transition layer at interface where bulk surfactant concentration gradient ∇C is large.

$$Pe = \frac{Ua}{D} \approx 10^6$$

- The accurate resolution of this layer is essential to evaluate the exchange of surfactant between interface and bulk flow.

- Hybrid numerical method
    - Analytical reduction of transition layer
    - Can be combined with boundary integral or other interfacial flow solver to efficiently compute at large Pe.

Governing equations

- We consider interfacial Stokes flow with bulk soluble surfactant in the exterior fluid

- The interfacial surfactant concentration Γ and bulk surfactant concentration C satisfy advection-diffsion equations

$$\frac{\partial \Gamma}{\partial t}\bigg|_\xi - \frac{\partial \boldsymbol{X}}{\partial t}\bigg|_\xi \cdot \nabla_s \Gamma + \nabla_s \cdot (\Gamma \boldsymbol{u}_s) + \Gamma \kappa u_n = \frac{1}{Pe_s}\nabla_s^2 \Gamma + J\boldsymbol{n} \cdot \nabla C\big|_S \ , \quad \boldsymbol{x} \in S \ \ ;$$

$$\frac{\partial C}{\partial t} + \boldsymbol{u} \cdot \nabla C = \frac{1}{Pe}\nabla^2 C \,, \qquad x \in \Omega_2$$

- Boundary and far-field conditions are

$$J\mathbf{n} \cdot \nabla C \mid_S = Bi(K(1 - \Gamma)C \mid_S -\Gamma)$$

$$C \to 1 \ \text{ as } |\boldsymbol{x}| \to \infty$$

- The surfactant concentration couples to the fluid dynamics through the stress balance:

$$-(p_2 - p_1)\mathbf{n} + 2(\mathbf{e}_2 - \lambda \mathbf{e}_1) \cdot \mathbf{n} = \sigma \kappa \mathbf{n} - \nabla_s \sigma, \qquad \lambda = \frac{\mu_1}{\mu_2}$$

$$\text{where} \ \ \sigma = 1 + E \ln(1 - \Gamma)$$

4

The large bulk Peclet number limit

- We use singular perturbation analysis to derive a reduced asymptotic model for $Pe \gg 1$.

- The 'outer' region, where spatial gradients are not large, is characterized by a regular approximation. In the limit $Pe \gg 1$, to leading order,

$$(\partial_t + \boldsymbol{u} \cdot \nabla)C = 0,$$

so that C is constant on particle paths, i.e., $C \equiv 1$ over much of Ω_2 for $t \geq 0$.

- When the drop deforms, local change of its interfacial area causes the surface surfactant concentration Γ to depart from its initial equilibrium value Γ_0.

- Slow diffusion of bulk surfactant causes large spatial gradients of C to develop in the normal direction close to the interface.

- In this "transition" region, we introduce a surface fitted coordinate system (ξ_1, ξ_2, n) and stretched coordinate $N = n/\epsilon$ with $\epsilon = Pe^{-1/2}$, and find to leading order

$$(\partial_t|_n + \boldsymbol{u}_s \cdot \nabla_s + \partial_n v_p|_s N \partial_N)C = \partial_N^2 C$$
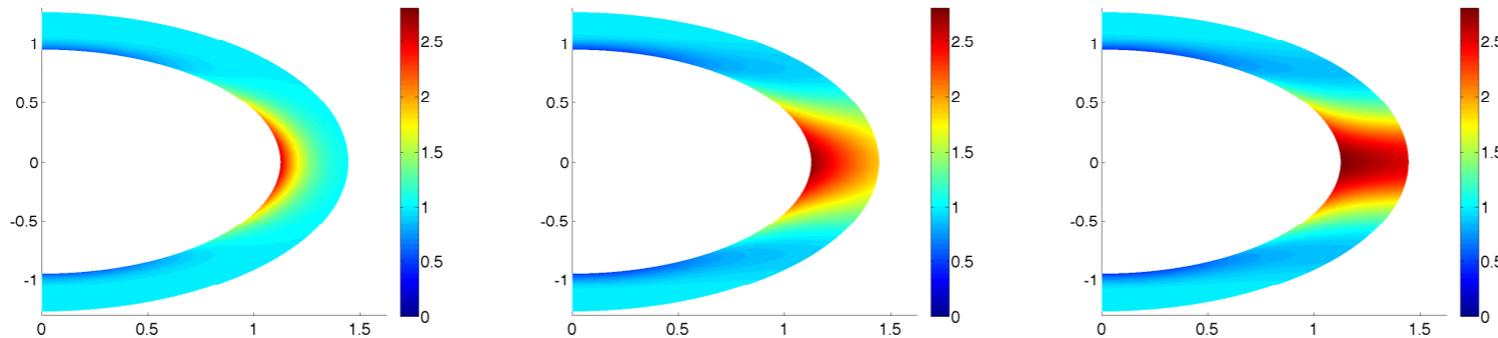
$$\text{where} \quad \partial_n v_p|_s = -\kappa u_n - \nabla_s \cdot \boldsymbol{u}_s, \quad \text{ι} \, \partial_t - \partial_t \boldsymbol{X}|_{\boldsymbol{\xi}} \cdot \nabla_s = \partial_t|_n$$

Other details

- The boundary conditions for the transition layer equation are

$$J_0 \partial_N C|_s = Bi(K(1-\Gamma)C|_s - \Gamma) \ \text{ on } N = 0,$$

$$\text{and as } N \to \infty \begin{cases} C \to 1 & \text{when } \partial_n v_p|_s \leq 0, \\ \partial_N C \to 0 & \text{when } \partial_n v_p|_s > 0. \end{cases}$$

- There is no transition layer in the velocity.

- Error in the approximatiion is $O(\epsilon)$.

- The hybrid method conserves surfactant at $O(\epsilon)$, with a remainder of $O(\epsilon^2)$.

Advantages of hybrid numerical method

- Pe removed from problem at leading order. In plots, we reintroduce Pe via $n = Pe^{1/2}N$.

- We use a fixed rectangular grid or mesh-free method for the numerical solution for C, combined with simultaneous BI solution for $\mathbf{u}, \Gamma$.

- No need to remesh grid for C as interface evolves, even for highly contorted interface shapes

- Diffusive term $\partial_N^2 C$ is $O(1)$, so no development of large concentration gradients that require a large number of node points to resolve

- $\mathbf{u}$ need only be evaluated at interface

Boundary integral method

- The equations are solved by a boundary integral method, and a finite difference method (on a rectangular domain) is used for the transition layer equation

- The inclusion of baffles introduces two additional single layer integrals.

- In the axisymmetric geometry, azimuthal integrations can be done analytically, reducing surface integrals to line integrals.

- We use Alpert hybrid Gauss-trapezoid quadrature for logarithmic kernel singularities, a method of Ceniceros et al. to reduce round off error amplification in computation of single and double layer potentials, and adaptive point insertion.

- Full method is $O(h^2)$ on the drop interface, $O(h)$ on the baffles (due to the singularity of the flow around the sharp aperture edges), and $O(\Delta t)$.

Error in the axial
and radial components
of the double-layer potential
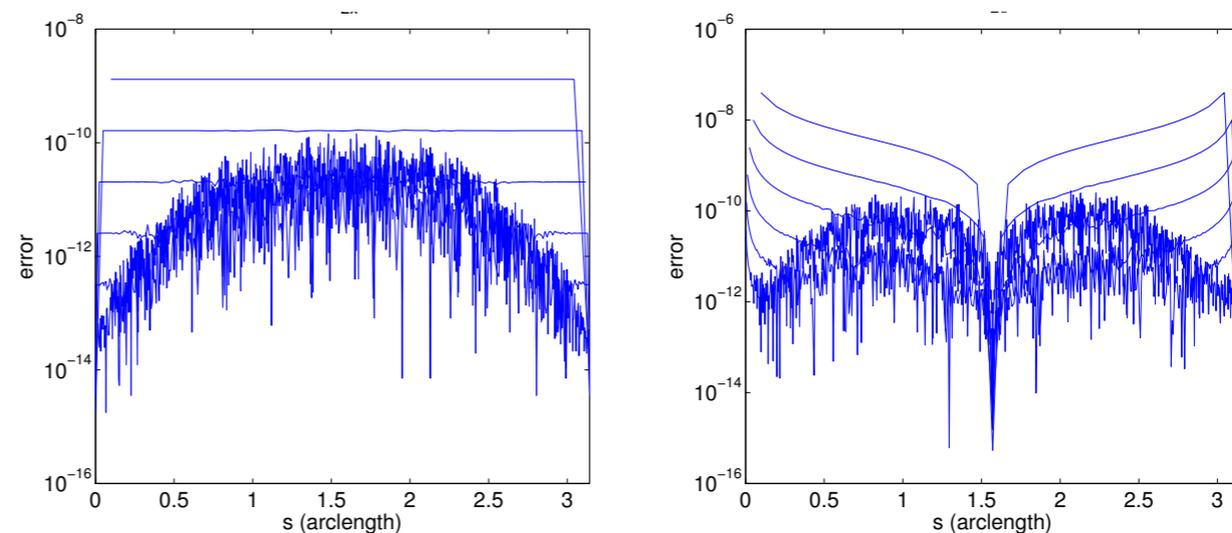
Error versus arclength for $n = 32, 64, 128, 256, 512, 1024$.

Boundary integral formulation

$$u_j(\boldsymbol{x}_0) - \frac{1-\lambda}{4\pi(1+\lambda)} \int_S^{\mathcal{PV}} u_i(\boldsymbol{x})T_{ijk}(\boldsymbol{x},\boldsymbol{x}_0)n_k(\boldsymbol{x})dS(\boldsymbol{x}) + \frac{1}{4\pi(1+\lambda)} \int_{S_b} G_{ij}(\boldsymbol{x},\boldsymbol{x}_0)g_i(\boldsymbol{x})dS(\boldsymbol{x})$$

$$= \frac{2}{1+\lambda}u_j^\infty(\boldsymbol{x}_0) - \frac{1}{4\pi(1+\lambda)} \int_S G_{ij}(\boldsymbol{x},\boldsymbol{x}_0)[\sigma_{ik}(\boldsymbol{x})]_1^2 n_k(\boldsymbol{x})dS(\boldsymbol{x}), \quad \boldsymbol{x}_0 \in S \,,$$

$$\frac{\lambda-1}{8\pi} \int_S u_i(\boldsymbol{x})T_{ijk}(\boldsymbol{x},\boldsymbol{x}_0)n_k(\boldsymbol{x})dS(\boldsymbol{x}) + \frac{1}{8\pi} \int_{S_b} G_{ij}(\boldsymbol{x},\boldsymbol{x}_0)g_i(\boldsymbol{x})dS(\boldsymbol{x})$$

$$= u_j^\infty(\boldsymbol{x}_0) - \frac{1}{8\pi} \int_S G_{ij}(\boldsymbol{x},\boldsymbol{x}_0)[\sigma_{ik}(\boldsymbol{x})]_1^2 n_k(\boldsymbol{x})dS(\boldsymbol{x}), \quad \boldsymbol{x}_0 \in S_b \,.$$

- The stokeslet and stresslet Green's functions are

$$G_{ij}(\boldsymbol{x},\boldsymbol{x}_0) = \frac{\delta_{ij}}{r} + \frac{\hat{x}_i\hat{x}_j}{r^3} \quad \text{and} \quad T_{ijk}(\boldsymbol{x},\boldsymbol{x}_0) = -6\frac{\hat{x}_i\hat{x}_j\hat{x}_k}{r^5}$$
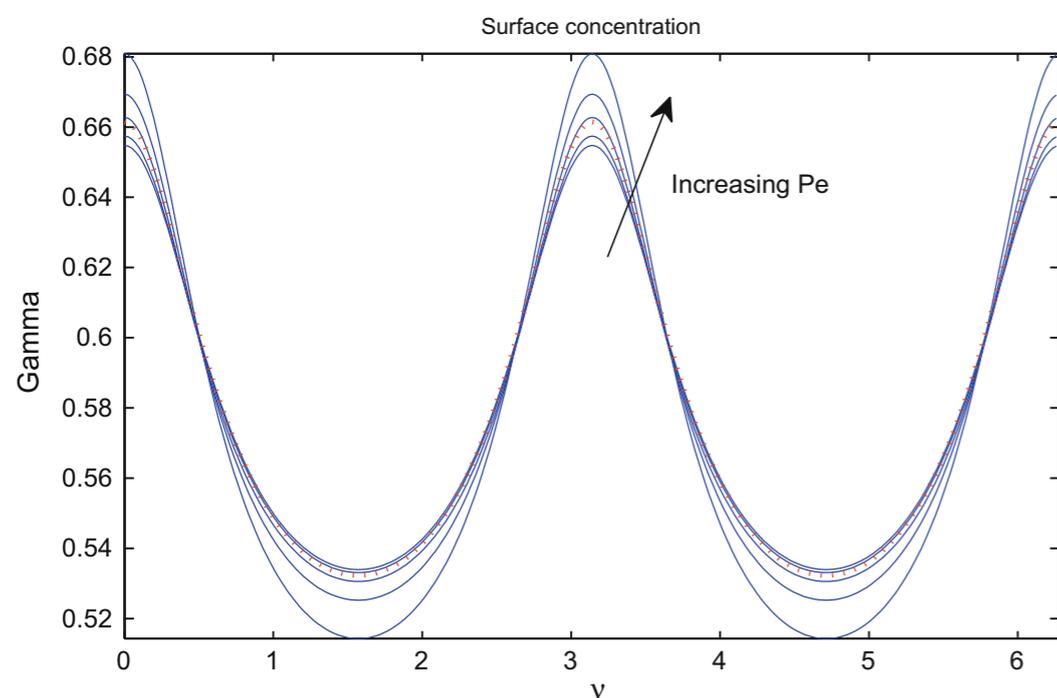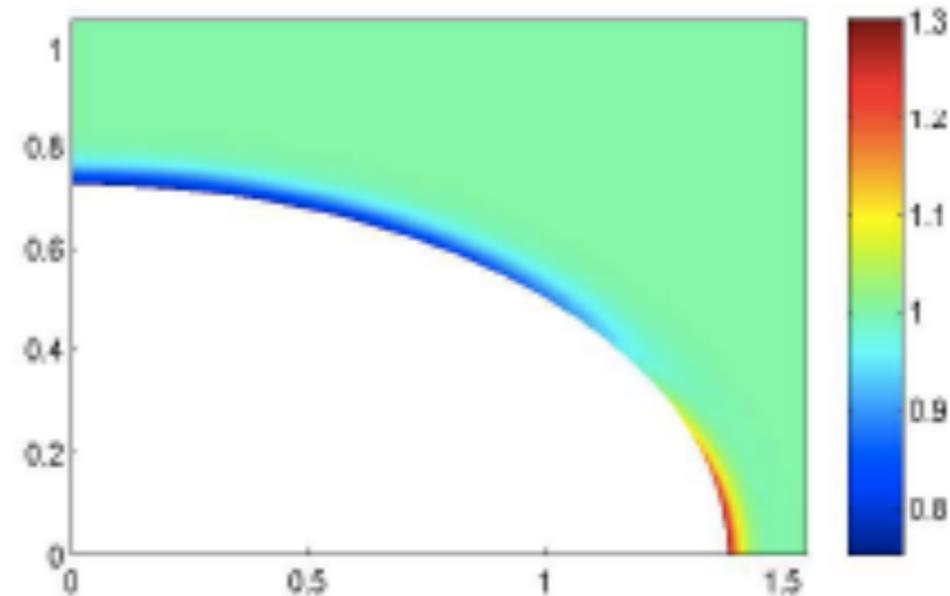
where $\hat{\boldsymbol{x}} = \boldsymbol{x} - \boldsymbol{x}_0$ and $r = |\hat{\boldsymbol{x}}|$.

Validation (Booty & Siegel 2010)

Hybrid $Pe = 10^3$

'Traditional', $Pe = 10^3$

Surface concentration

Increasing Pe
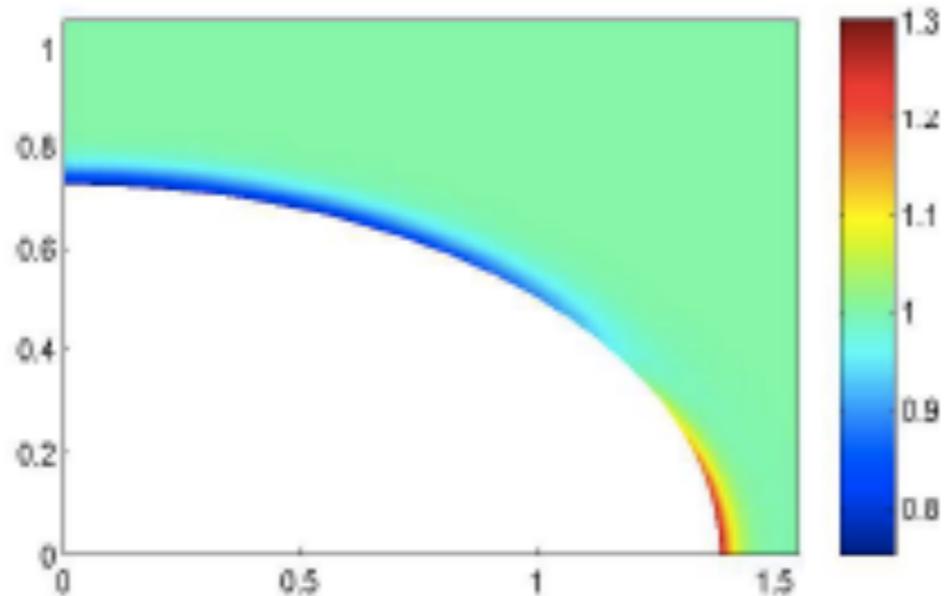
Surface concentration
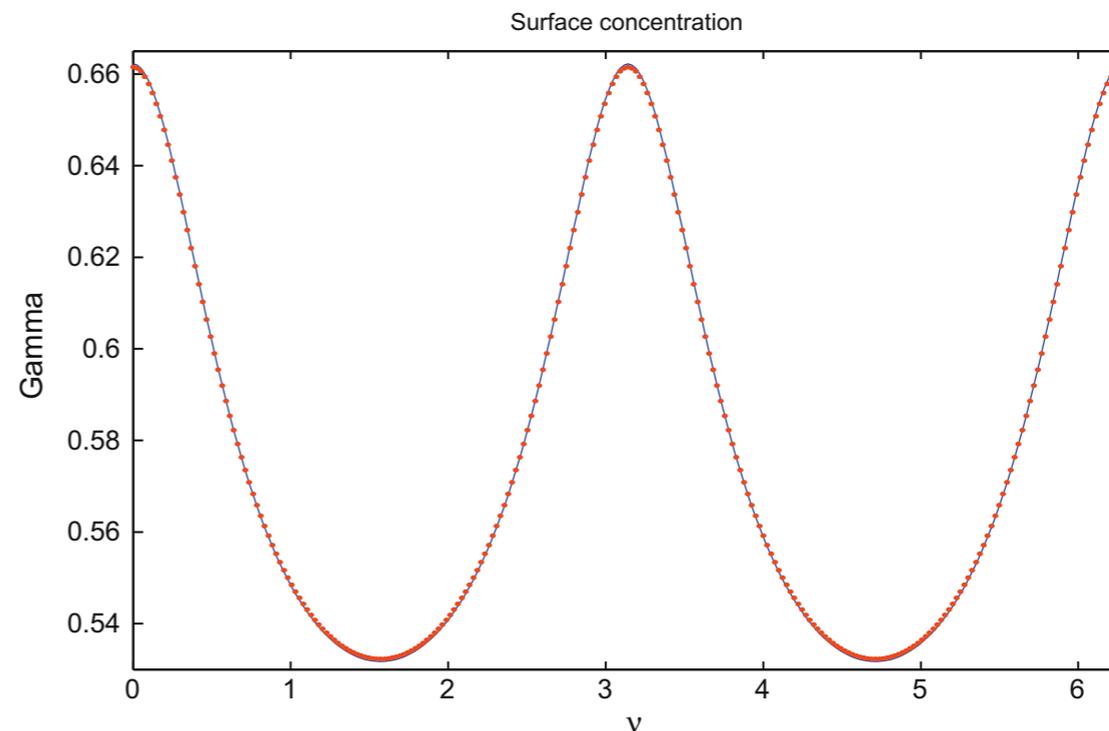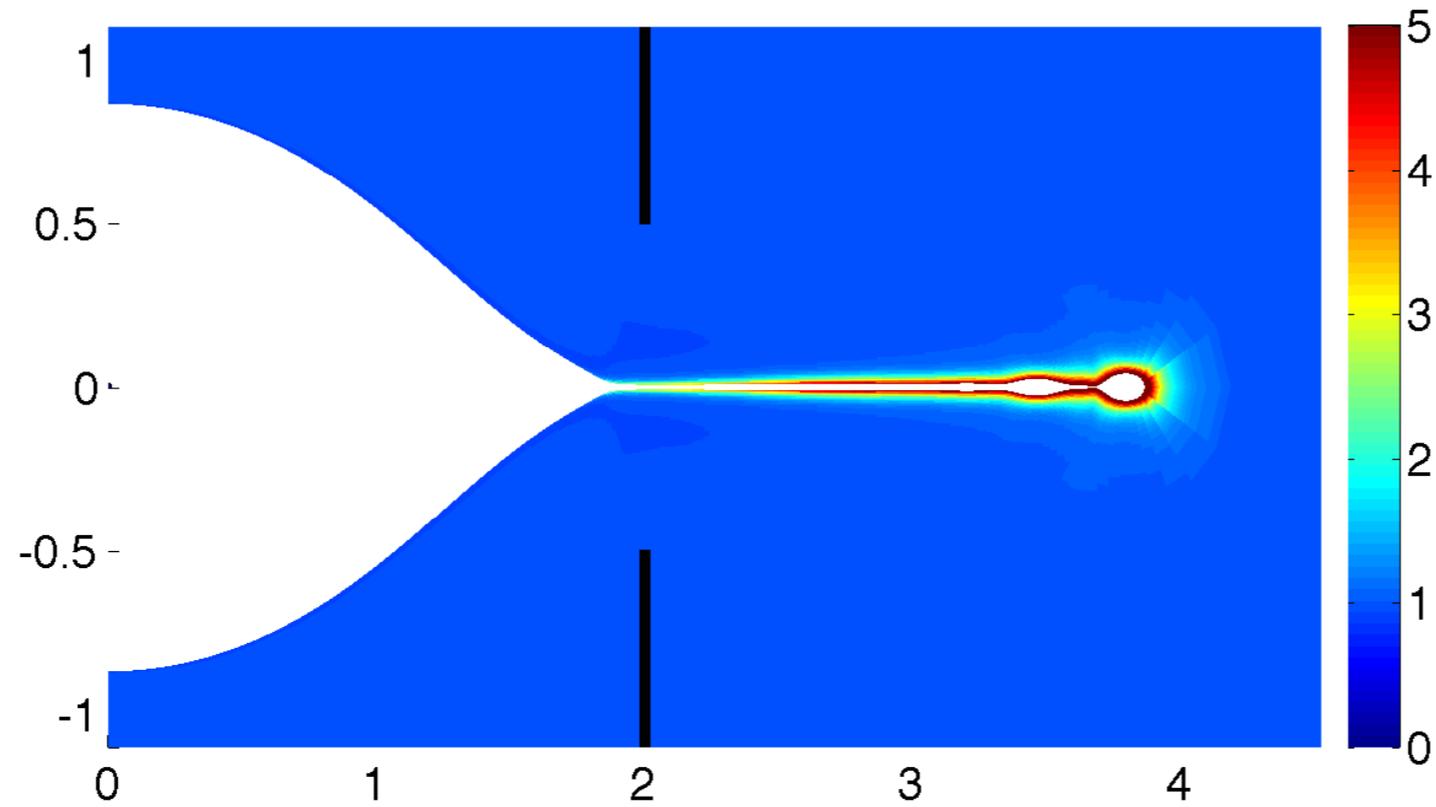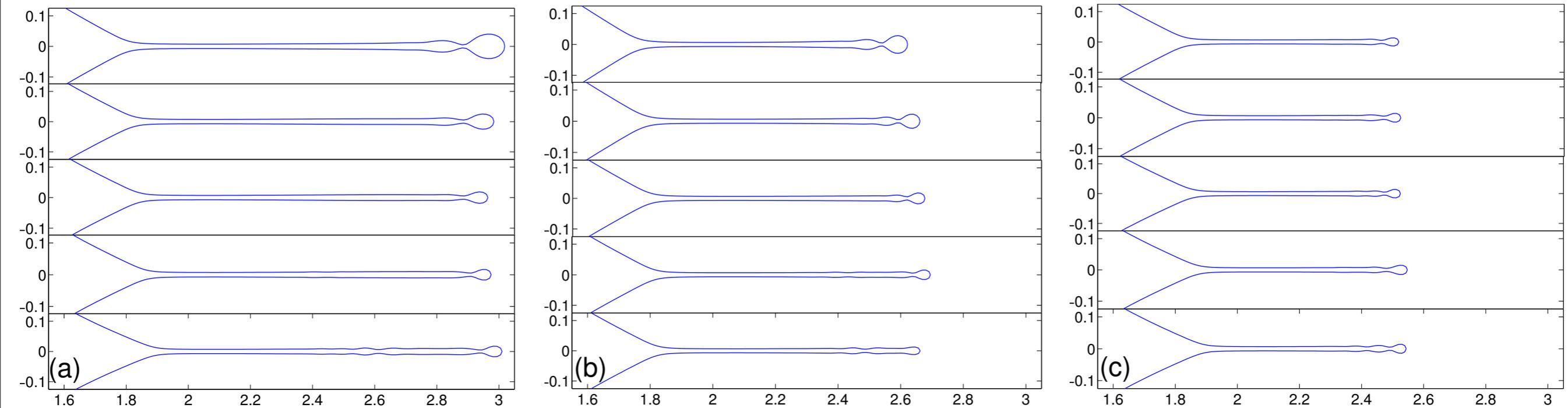

Left: Surface concentration Γ computed by the hybrid method (dotted red curve) and by the traditional method (solid blue curves) for $Pe = 0.5 \times 10^2, 10^2, 10^3, 10^4$, and 0.5×10^5. Right: adaptive resolution applied to $Pe = 10^4$.
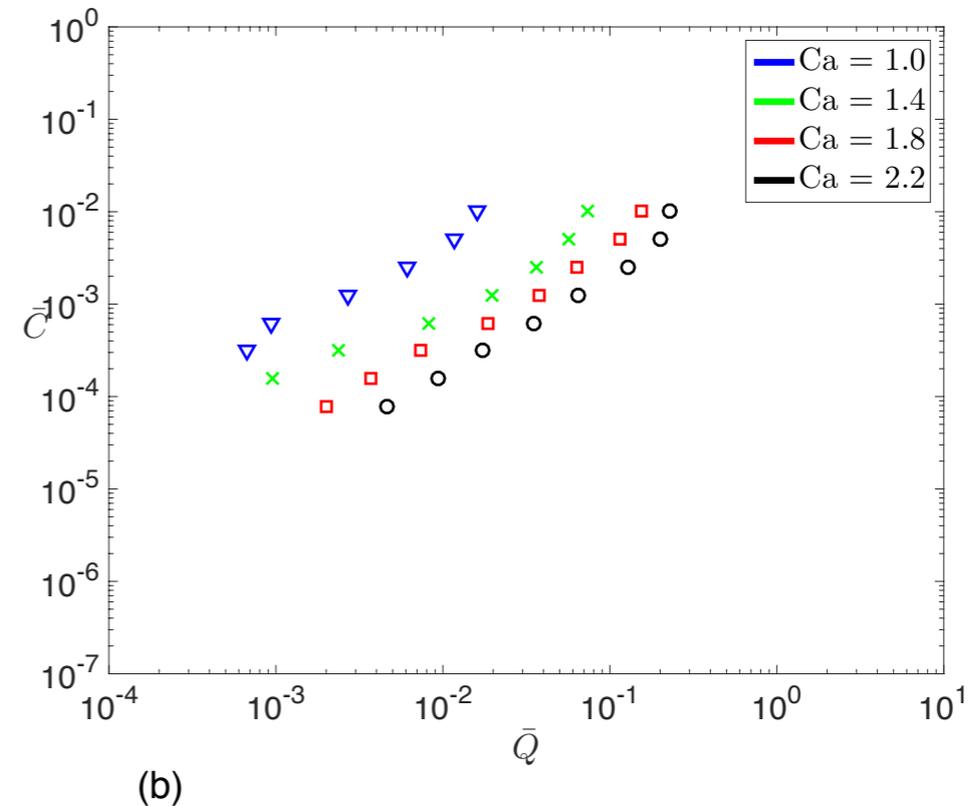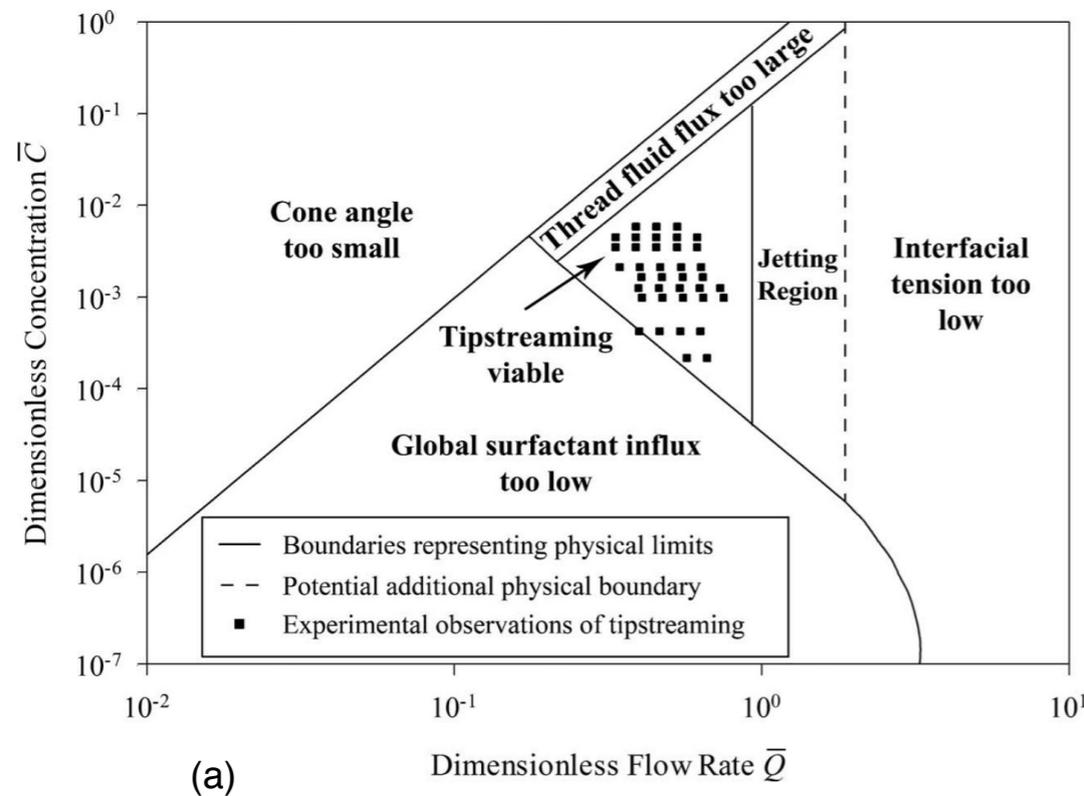
Numerical results

Example of a tipstreaming thread with $Bi = 0.1, r_0 = 0.50, Ca = 1.82,$ and $\Gamma_0 = 0.10.$ Spatial data for C is displayed using $Pe = 10^4.$

Thread evolution with aperture radius $r_0 = 0.50$, $Ca = 1.82$, and $\Gamma_0 = 0.10$. (a) $Bi = 0.25$, the time interval between frames is $\Delta t = 0.3$ with the first (top) frame at $t = 8.4$. (b) $Bi = 0.50$, the frame time interval is $\Delta t = 0.3$ with the first (top) frame at $t = 7.8$, continued by (c) where the frame time interval is $\Delta t = 0.2$ with the first (top) frame at $t = 9.2$.

Conditions for tipstreaming

(a)

(b)

The simulations closely replicate the experimental values of J0 and BiK, but at larger values of Bi and smaller values of K, and so it is expected that the relative importance of adsorption is maintained while the role of desorption is enhanced

Dimensionless quantity	Value in experiments	Value in simulations
Baffle location, $x = l = \Delta Z/a$	2.02	2.0
Aperture radius, $r_0 = w_{or}/2a$	0.20	0.50
Viscosity ratio, $\lambda = \mu_1/\mu_2$	0.025	0.050
Elasticity number, $E = RT\Gamma_\infty/\sigma_0$	0.09	0.20
Peclet numbers, $Pe_s \simeq Pe = Ua/D$	1.46×10^6	$Pe_s = 10^3$
Expansion parameter, $\epsilon = Pe^{-1/2}$	0.83×10^{-3}	−
Exchange coefficient[a], $J = DC_\infty/\Gamma_\infty U$	4.30×10^{-7} to 4.30×10^{-5}	−
Scaled exchange coefficient[a], $J_0 = J/\epsilon$	5.18×10^{-4} to 5.18×10^{-2}	7.8×10^{-4} to 10^{-1}
Biot number, $Bi = a\kappa_d/U$	4.16×10^{-10}	10^{-3}
Partition coefficient[a], $K = \kappa_a C_\infty/\kappa_d$	4.83×10^4 to 4.83×10^6	1.56×10^{-2} to 2.0
Modified Biot number[a], BiK	2.0×10^{-5} to 2.0×10^{-3}	1.56×10^{-5} to 2.0×10^{-3}

- Rescaling the simulation data for $\bar{Q}$ to account for the different aperture radius between experiments and simulation puts it in the range $\bar{Q} \in (0.016, 3.13)$

Highly accurate simulations of surfactant-laden drops in 2D Stokes flow

- We use a complex variable formulation of boundary integral equations, following Kropinski (2001)

- Spectral accuracy in space and the adaptive time-stepping scheme allows for control of the temporal errors

- A challenge is to maintain accuracy when drops are in close proximity

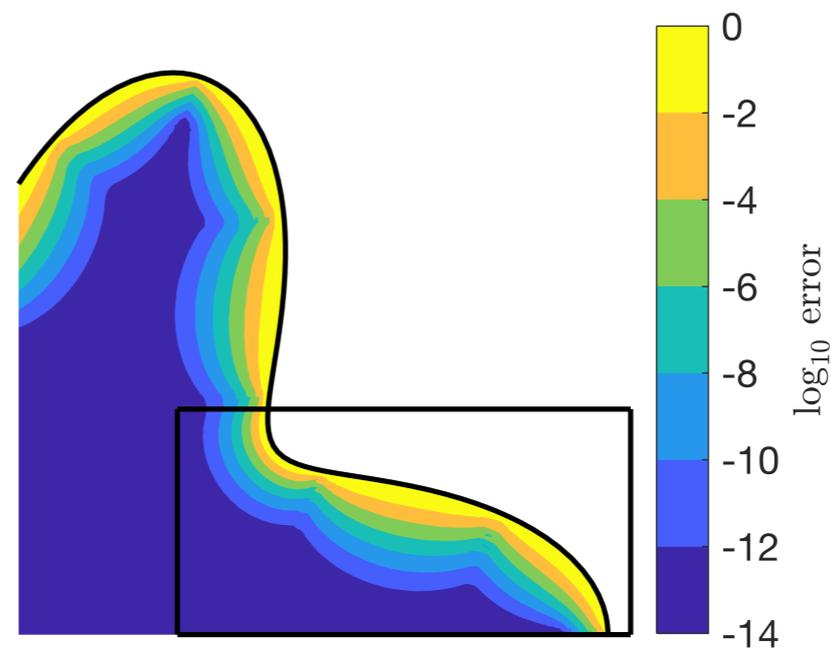- To address this, we employ a special quadrature, adapted from Helsing and Ojala (2008)
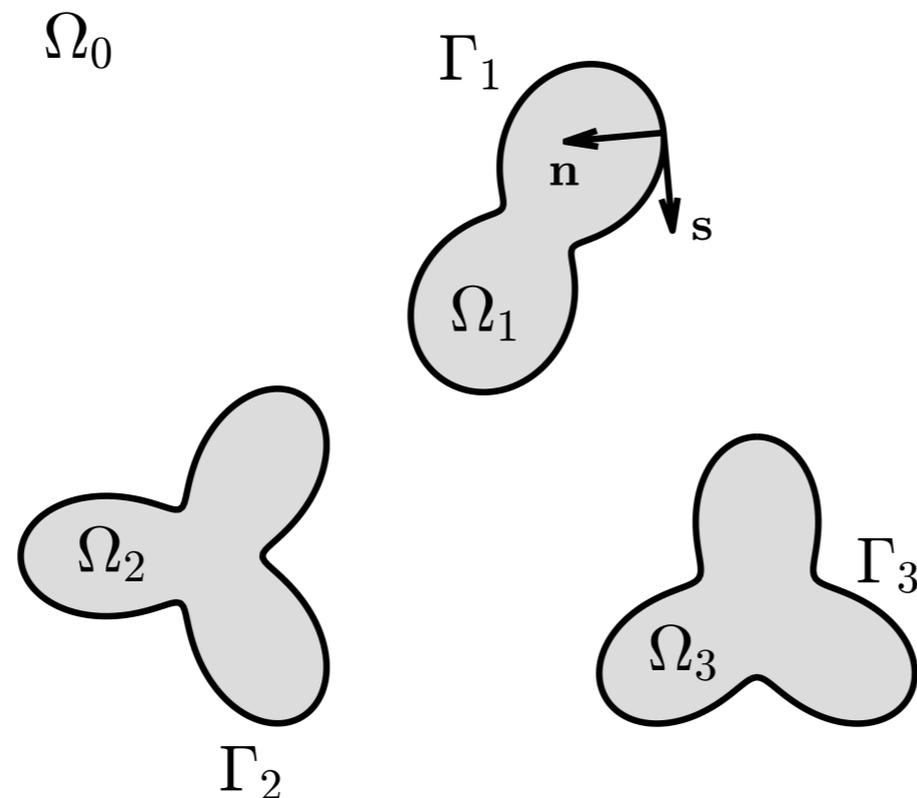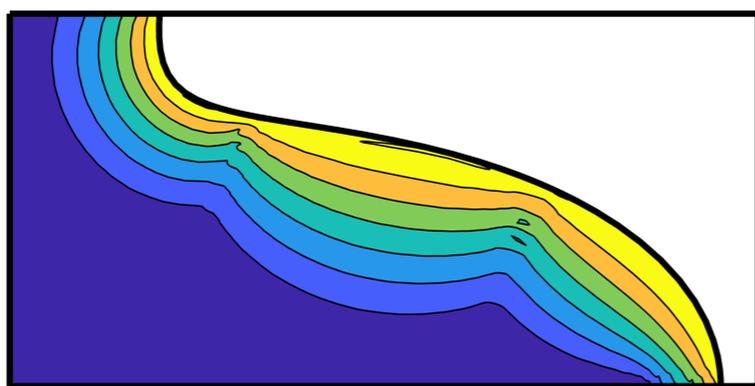
Near singular evaluation

- Compute, e.g., $\int_\Gamma \frac{f(\tau)d\tau}{\tau - z}$ for z near Γ
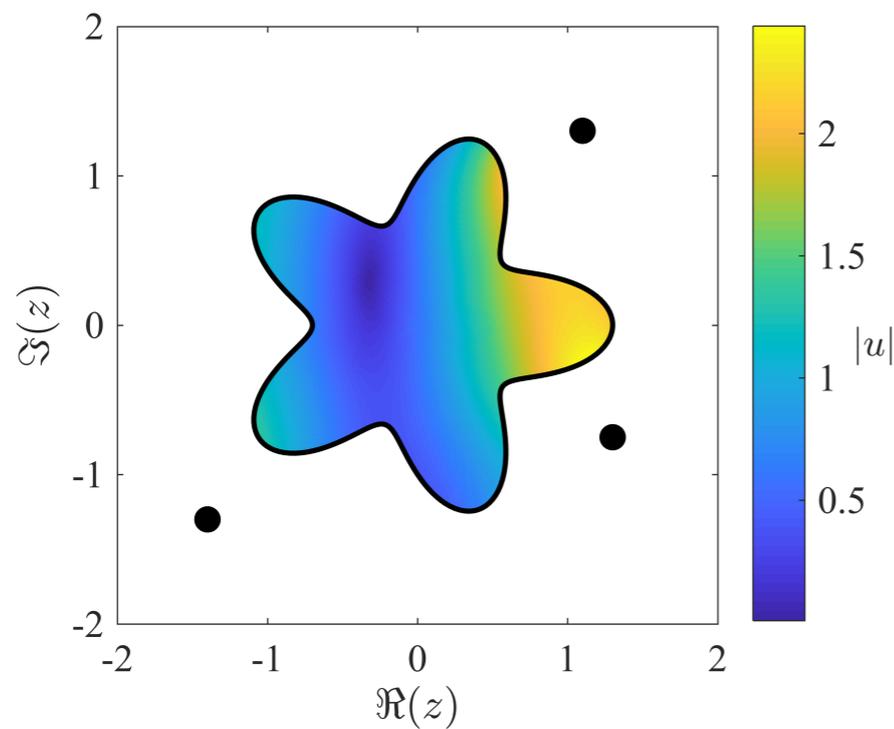
(a) Domain Ω, source points and solution $u(z)$.

(b) Error in first quadrant of domain.

(a) 25 panels
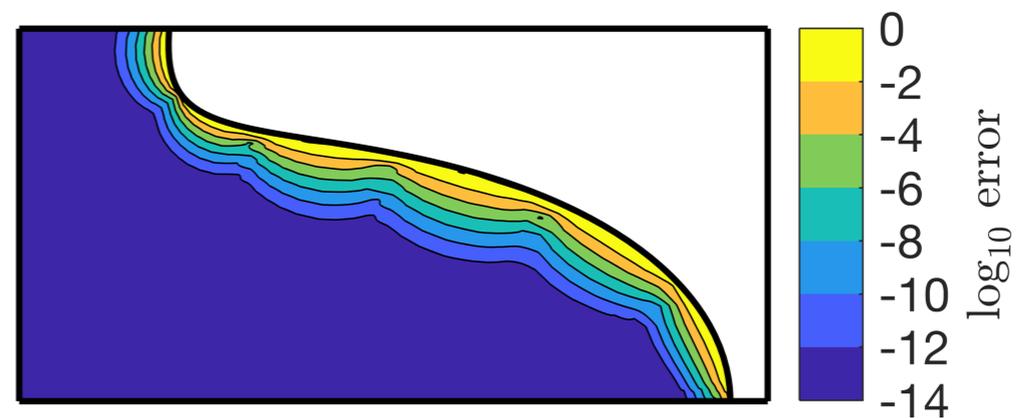
(b) 50 panels

Figure 3: Computed error estimates in black for error levels 10^{-p}, where $p = 14, 12, \ldots, 2, 0$. Measured errors in colour.

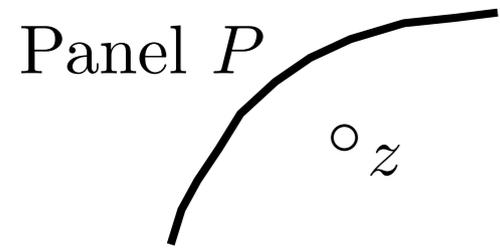# Special quadrature

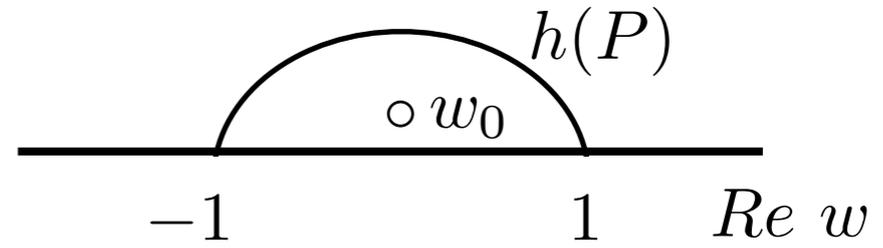- Based on composite Gauss-Legendre quadrature
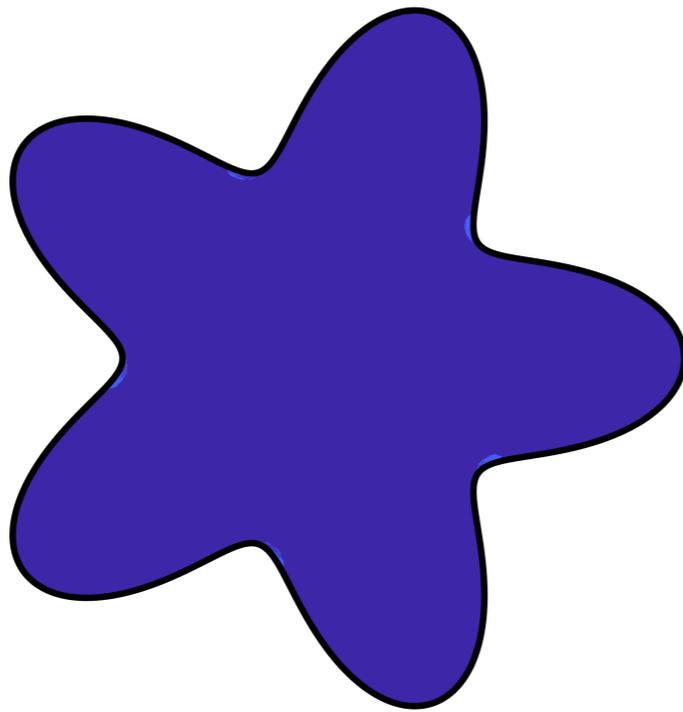
(a) Error in whole domain.
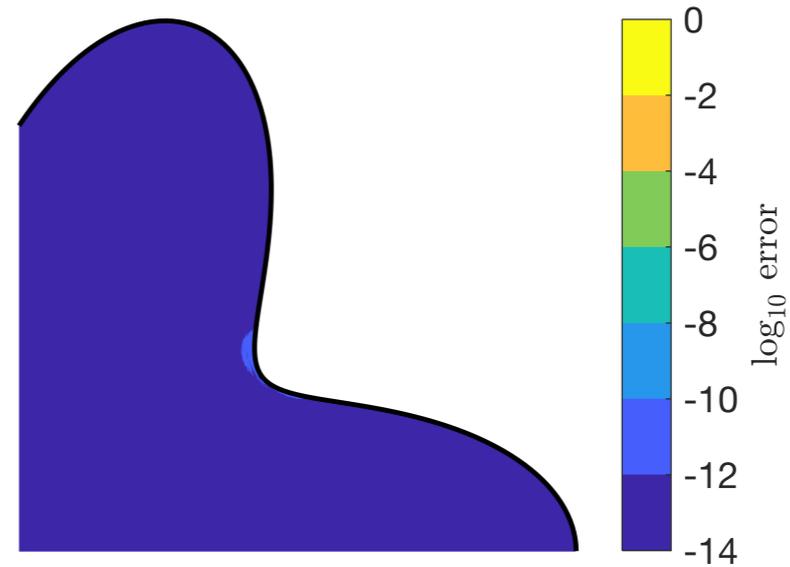
(b) Error in first quadrant.

Logarithm of error when solving Stokes equations using special quadrature for evaluating at points close to the boundary

Special quadrature

Panel P $w = h(\tau)$ $h(P)$

$\circ\, z$ $\longrightarrow$ $\circ\, w_0$

                                           -1 1 $Re\ w$

$$
\int_P \frac{f(\tau)}{\tau - z}\, d\tau \;=\; \int_{h(P)} \frac{f(\tau(w))}{w - w_0}\, dw \tag{1}
$$

$$
=\; \int_{-1}^{1} \frac{\sum_{k=0}^{15} c_k w^k}{w - w_0}\, dw + residue \tag{2}
$$

$$
=\; \sum_{k=0}^{15} c_k \int_{-1}^{1} \frac{w^k}{w - w_0}\, dw + residue \tag{3}
$$

Computed analytically, using recursion formula

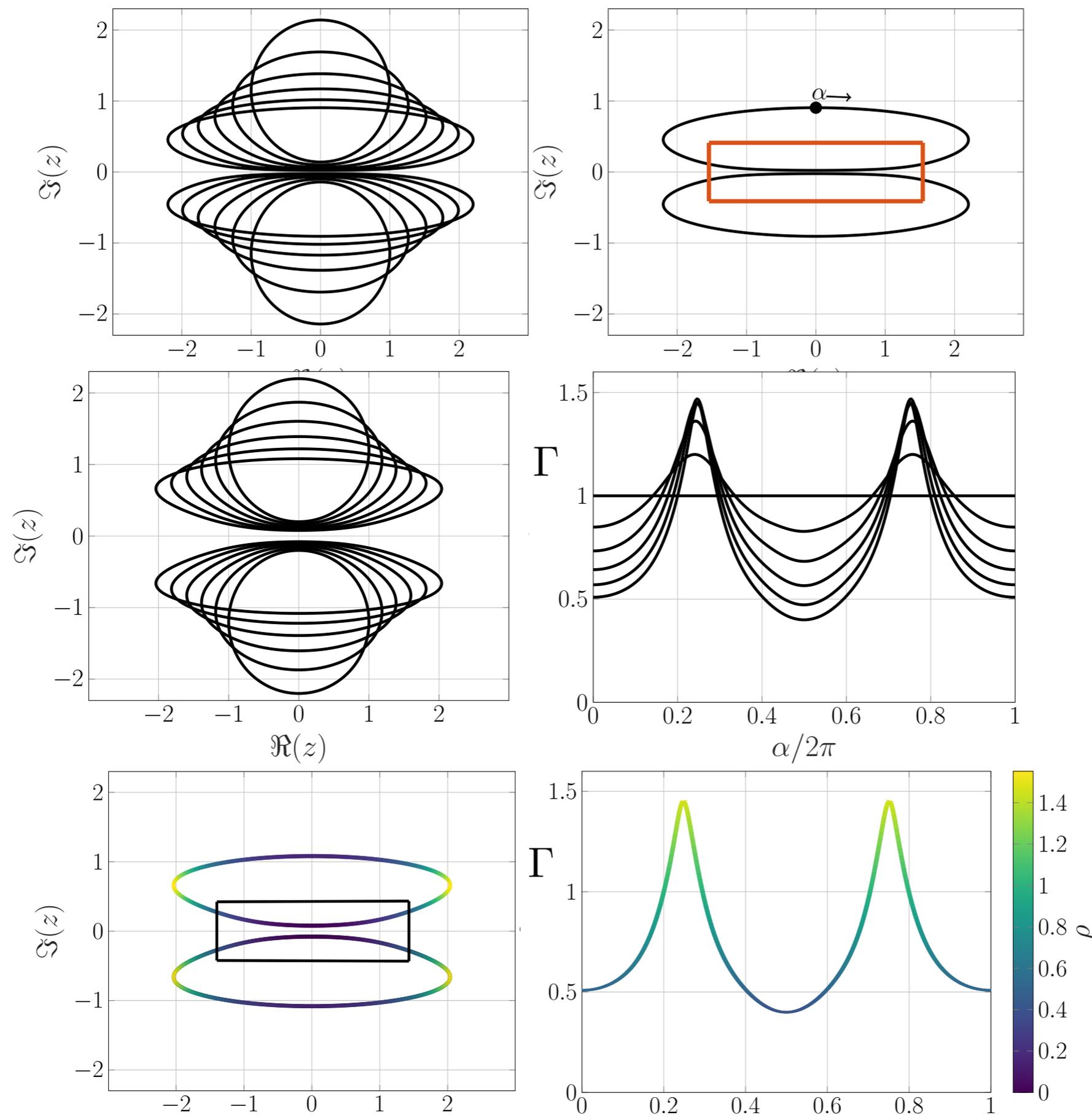Comparison with exact analytical solutions for insoluble surfactant (S. 1999)
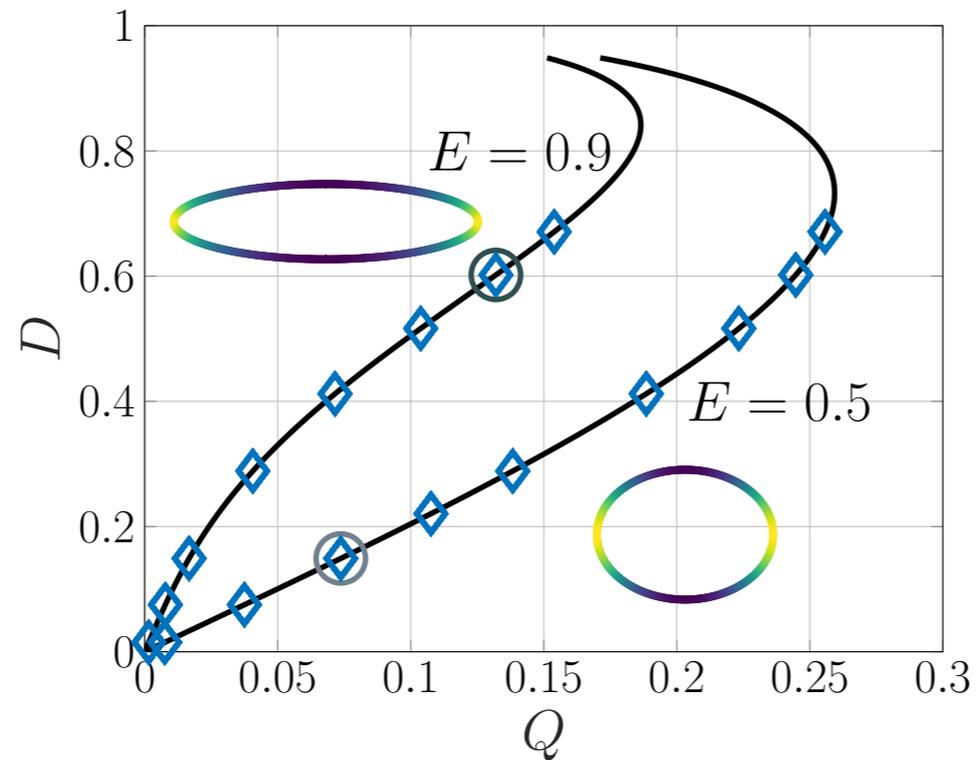
Deformation D vs.
Capillary number Q

Steady solution branches, theory (solid curve) and computations ($\diamond$)
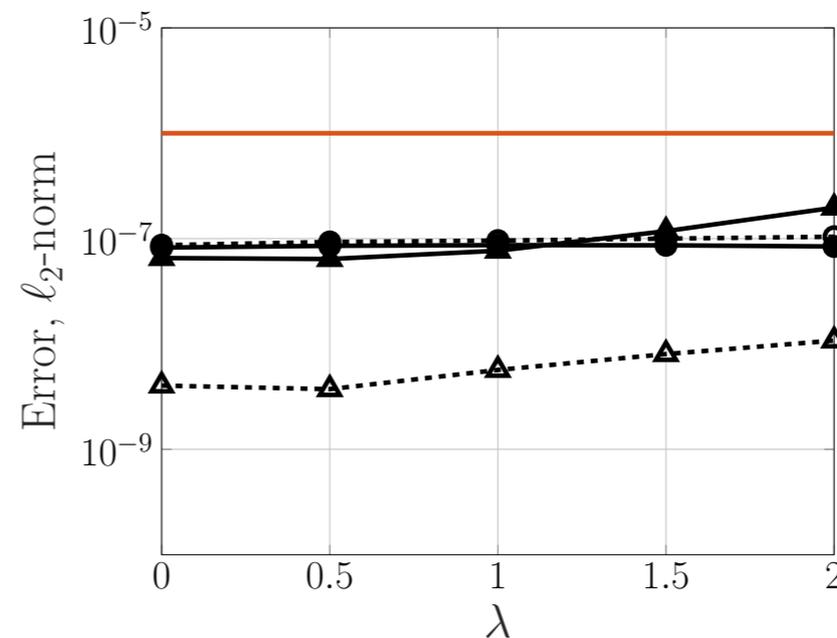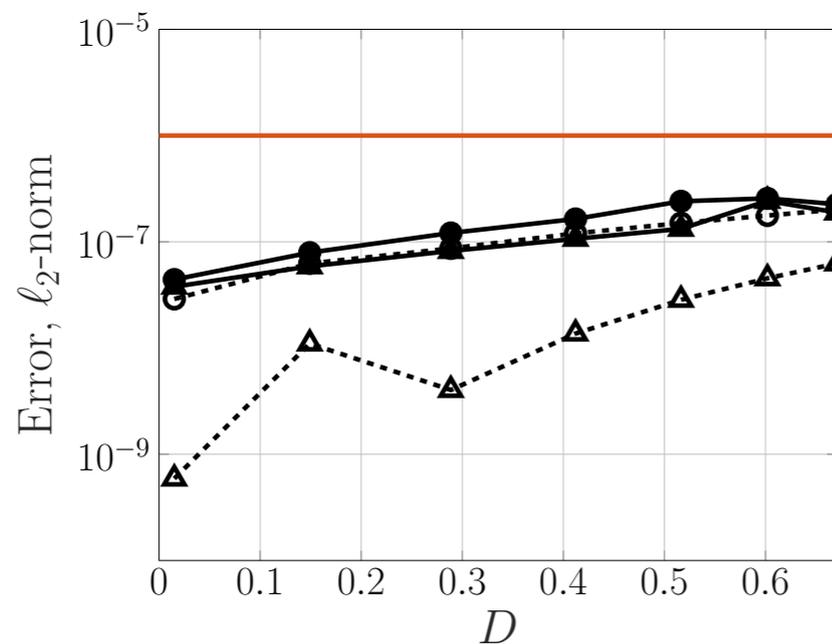
Error in interface shape and Γ, for $E = 0.5$ (solid lines) and $E = 0.9$ (dashed lines).
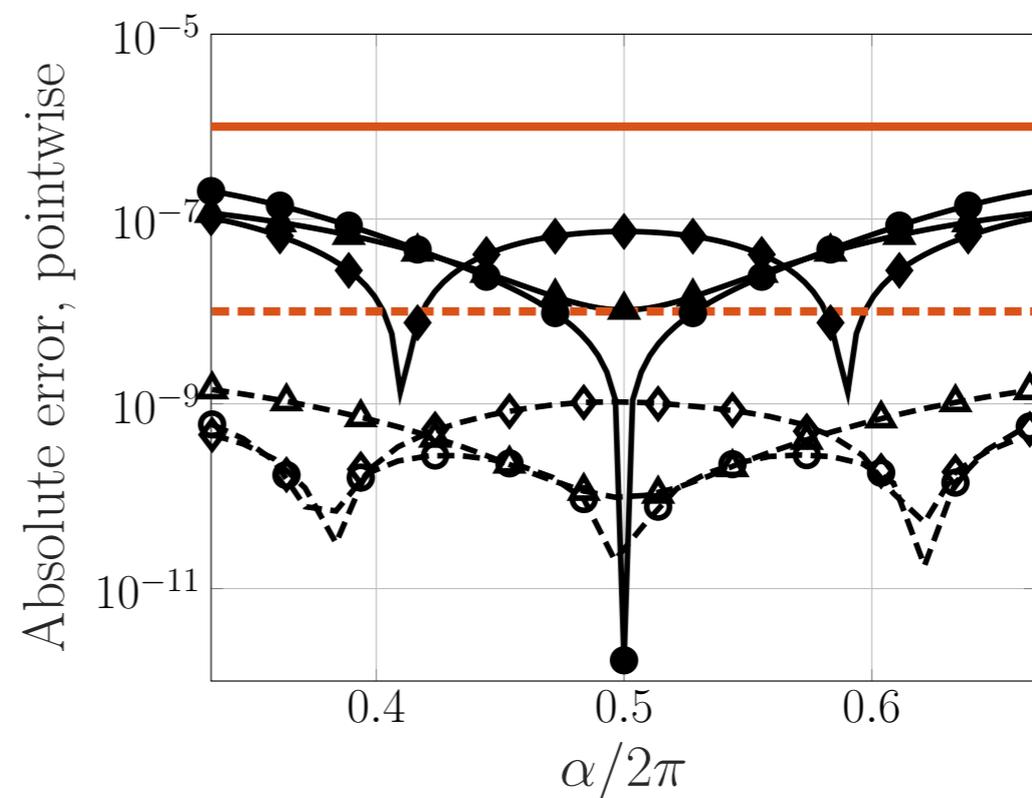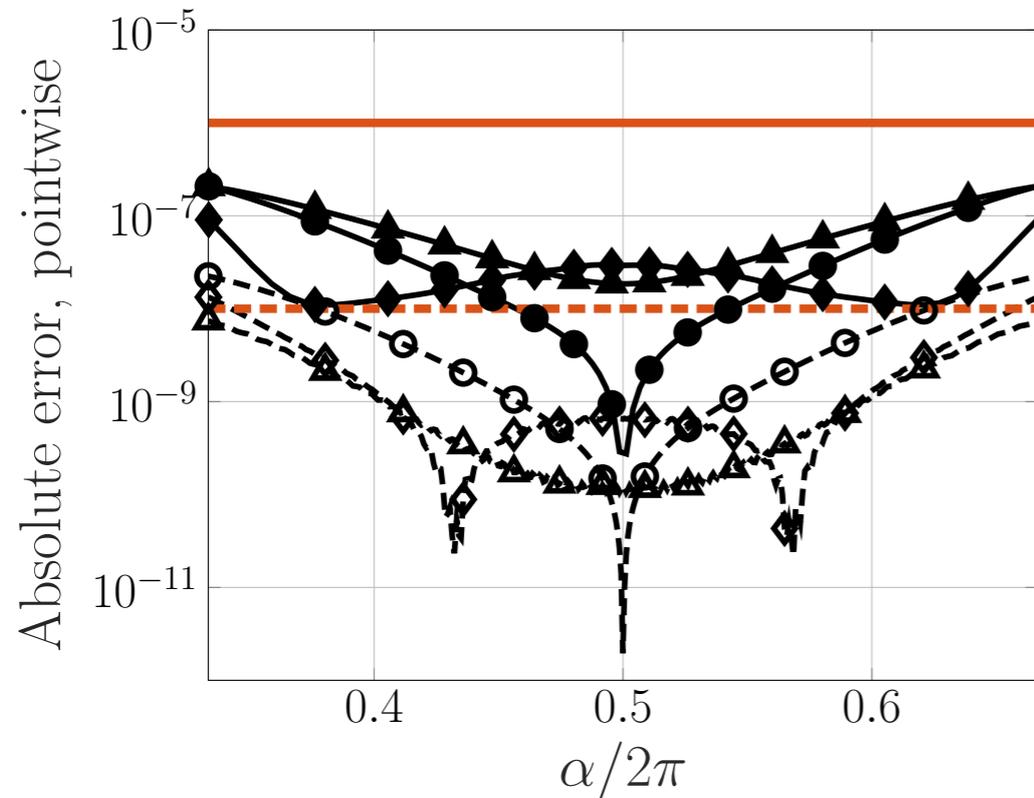
Two bubbles in a linear strain flow

Clean bubbles

With surfactant

Final time

Validation against a semi-analytic solution of Crowdy et al. (2005)

BIE method computed with 576 and 800 points per bubble respectively. Validation method computed with 2049 and 8193 points respectively. Markers: $\circ, \triangle, \diamond$ correspond to relative errors in x, y and Γ respectively
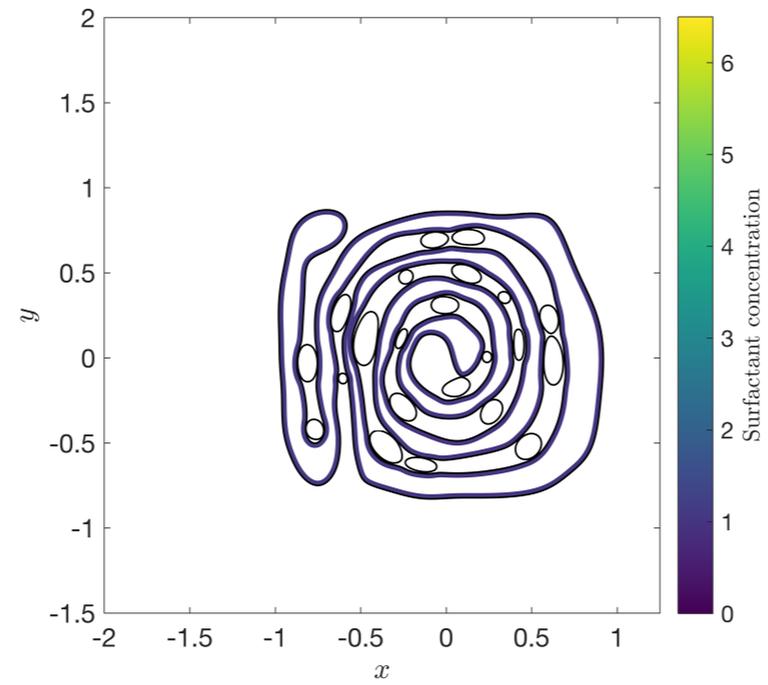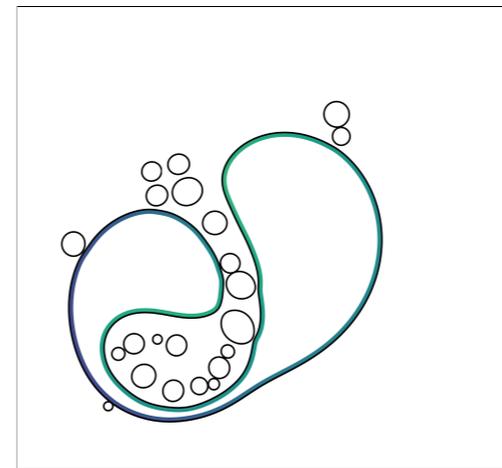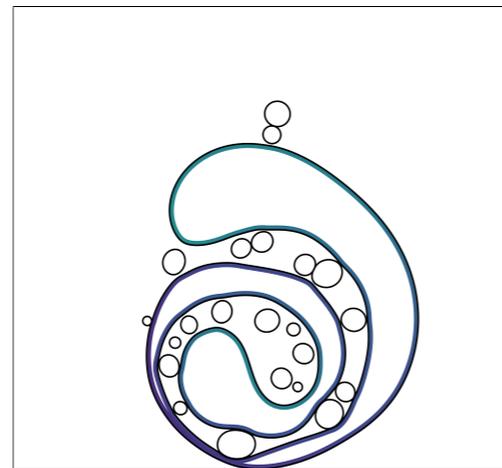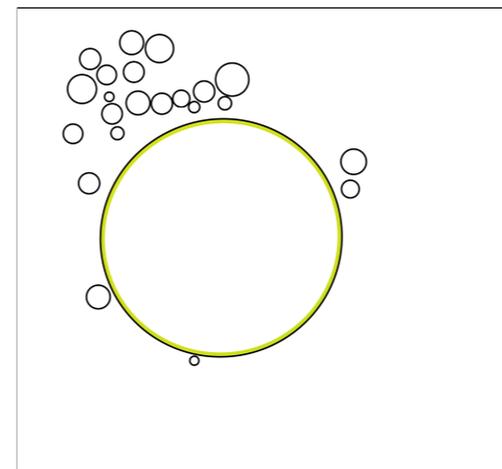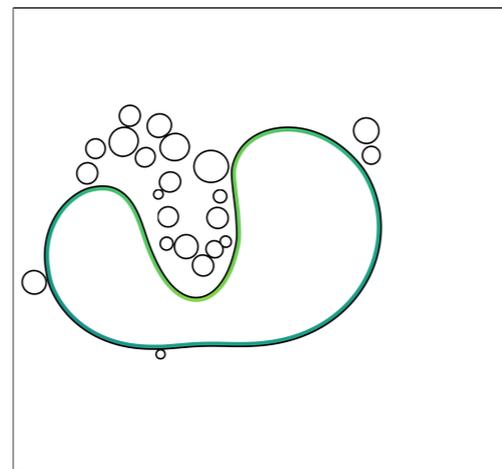
Final example: 'Swiss roll'

(a) $t = 2.5$

(b) $t = 5$

(c) $t = 10$

(d) $t = 20$

Conclusion

1. We have developed a numerical method that combines an asymptotic reduction in an interface-fitted coordinate system for $Pe \rightarrow \infty$ with a BI method for two-phase flow.

- The method is used to investigated the influence of geometric flow focusing on the tipstreaming of a drop that is facilitated by soluble surfactant.

- The flow focussing geometry is found to produce thinner fluid threads during tipstreaming, with a higher surfactant concentration.

2. We have developed a BI method for multiple surfactant-laden drops in two-dimensional flow, that retains high accuracy when drops are close together.

- The method was validated by comparing to exact analytical solutions for a single drop and semi-analytical solutions for two drops in straining flows.